

Discussion

This Dissertation looked at the residence time in a coastal plain estuary. Two modeling techniques were established and compared, and several model and data sets were evaluated until a realistic simulation of the estuary in question could be produced. This simulation acted as the baseline case which was compared to several modeling runs where the primary forcing parameters could be varied to show the relative importance of each, to the spatial patterns and overall residence time.

The majority of the effort in modeling studies of this kind, where the target outcome depends on an accurate simulation of fluid flow, is in the meticulous setup, calibration, and validation of the model over the domain and time period in question. This results in the requirement of high quality data from many locations over a time period sufficient to answer the question posed. In Tampa Bay with the PORTS and COMPS systems and the TOP study, together with the availability of EPC salinity data, USGS stream flow data, and NWS rain gage data, over long (order years) time periods, it was possible to adjust the free parameters in the model until a very close agreement between model output water level, current, and salinity was achieved over both short and long time scales. These data were then supplemented with real-time drifter data and the now-cast forecast system via TRACKER to verify that the modeled particle paths agreed with real drifter

trajectories, at least for short-term, sub-grid scales. Since the sub-grid scale dispersion is the only free parameter in the particle advection subroutine, this agreement is the most important; and it constitutes a first approximation to a longterm statistical agreement.

The FMDS opened the door to the possibility of a tractable definition for residence time that could vary in time and space over an estuary. It also provided key insight into the difficulties associated with data collection, model validation, diffusion schemes, particle trajectory validation, and sub-grid scale dispersion. It also gave results in the form of particle tracks versus concentration gradients that suggested a comparison between the two methods. The FMDS provided data that lead to a dispersion coefficient, and to a finer grid for the model as well as clarifying the need for better freshwater input for accurate simulations.

The SMDS was much improved in that it employed a finer grid which is near the lower limit in size to cover the domain and meet the CFL condition and still run longterm simulations in a reasonable time period. It employed a more realistic freshwater inflow (in both the number and location and temporal resolution of rivers) precipitation input and evaporation estimates at the surface boundary. The SMDS also utilized the embedded particle advection subroutine and passive tracer subroutine, which allowed for much longer runs in the same time period, while simultaneously reducing the model output files to a tractable size. The SMDS had the added advantage of TRACKER and an enhanced now-cast forecast system, together with an autonomous drifter program to verify its ability to capture the

sub-grid scale advection of the modeled particles. The SMDS was a first attempt at applying these modeling techniques to determine a residence time that has both spatial structure and temporal variance. The results show a spatial distribution of residence time for each of the Eulerian and Lagrangian based methods. The major difference in the Lagrangian and Eulerian methods is the strong spatial gradients in the cell-by-cell distributions of residence time of the former. This structure possibly results solely from the non-diffusive nature of the particle tracking method. The mouth of the bay region flushes very quickly. This is in agreement with the concentration method. However, there is a distinct region of low residence times along the deep navigational channel from the mouth up to the eastern head of the bay. Again this is in agreement with previous observations by Galperin et al., (1992b) that the residual advection of higher salinity waters from the shelf along the deep channels is the dominant longterm transport mechanism that maintains the salinity distribution in Tampa Bay. The sides of the bay show much longer residence times, implying that particles swept toward the bay edges accumulate behind the restriction of the causeways and irregularities in the bay geometry. These restrictions act as an impediment to outgoing particles, as well as providing an eddy structure for particle deposition.

In the Eulerian spatial distribution of residence time for the SMDS, the residence time gradients are too diffuse to see clearly; and the time series for the entire bay is very short (half), compared with the Lagrangian time series. These characteristics can be explained by the diffusion coefficient alone, indicating the

need for a model validation method that is sensitive to this parameter as was accomplished via the salinity validation.

In the TMDS which has the addition of salinity data from the EPC collection effort and the salinity data from the TOP study, modeled salinity compared well with observed salinity values in many locations throughout the bay. This skill, together with velocity and water level validation, lead to the reduction of the horizontal diffusion coefficient by a factor of ten. The close agreement between salinity data and modeled values over a wide range of time and space scales indicates a diffusion coefficient more in line with actual flow field dynamics.

Results from the Eulerian and the Lagrangian residence time comparison in the TMDS shows that the Eulerian method is smooth in space, having relatively small gradients in residence time over the domain. This is viewed as an oversimplification of the bay-wide residence time spatial distribution. In addition the Eulerian method is sensitive to the size of the diffusion coefficient, which needs to be adjusted to capture the salinity field in a realistic manner. In the case of Tampa Bay, this required the horizontal diffusion coefficient to be set to nearly zero introducing some numerical noise into the model. However, the model validation was still the best of any of the simulations. The Lagrangian method consistently showed a more detailed distribution of cell-by-cell residence times in both space and time, with steep gradients and persistent structure. Estimates by the Lagrangian method were similar to those of the Eulerian method in the length of the residence time for the whole bay for the TMDS. The Lagrangian method may be biased

toward sub-regions of the bay where particle numbers are over or under represented; however, agreement on bay-wide residence times between the two methods suggest otherwise.

The baseline case for the TMDS for both the Eulerian and Lagrangian approaches are good approximations to the cell-by-cell spatial distributions of residence time. They both show the lower bay, near the mouth, has a short residence time of less than 30 days. Because this region is dominated by the largest current velocities, the mechanism that dominates this region is likely distance to the open boundary divided by particle or water mass excursion (on the order of 10 kilometers per tide cycle during spring tides).

In the Eulerian distribution, the mid bay region shows smooth slight gradients from fewer than thirty days nearer the mouth to 90 - 120 days toward the eastern and western head of the bay, respectively. The Lagrangian distribution generally shows a similar structure, but has an area of longer residence time on the eastern side of the main shipping channel in the mid bay region. It also shows longer residence times along the bay edges, with a more pronounced tongue of low residence times that runs through the mid bay region from south-west to north-east. This region of the bay is where the horizontal density gradients tend to be highest and wind-induced currents from any direction except the north-east tend to trap particles along the bay edges. There is a strong depth dependence in this region, with shallower areas having longer residence times. This is consistent with the transverse nature of the baroclinic density-driven flow and also with the expected

surface stress and generally higher frictional effects in the shallower areas. This region is therefore not dominated by any one mechanism, but is controlled in time by the modulation of the various physical forces acting on the bay.

The eastern lobe of the upper bay shows very similar residence time characteristics when comparing the two methods. The Lagrangian estimates are uniform over the region with residence times around 90 days. In comparison, Eulerian residence times are approximately a month longer, but exhibit a similar uniform appearance. This is the region of the bay where the majority of the fresh water inflow is concentrated. The predominant contribution to the low residence times this far removed from the open boundary is likely large river input.

The western lobe of the upper bay is where the two methods differ most. This region is shallow and has little fresh water input from rivers. It also has three bridges with causeways and a constriction at its lower end. The Eulerian distribution shows very long residence times in this area (greater than 250 days). In comparison the Lagrangian distribution has isolated areas of very long (greater than 250 days) and broader areas of long (greater than 180 days) residence time. These occur mainly in the regions near the protruding causeways and shoreline, with regions between the causeways exhibiting low residence times. This spatial pattern is indicative of the barotropic pattern seen in the run where only the harmonic tides are used for forcing, implying that this shallow, confined region with little freshwater input is dominated by the gyre structure of the barotropic tides, and modulated by the other forces.

The bay could be broken into 4 distinct regions from looking at the residence time distributions from both methods. There is the region near the mouth of the bay that has low residence times regardless of the scenario or method. This region is dominated by its close proximity to the gulf, and tidal excursion alone can explain the short residence times. The mid bay region, where the salinity gradients are largest under normal conditions, does not seem to be dominated by any single mechanism. The river input and the wind stress both modulate the patterns in this region. The eastern lobe of the upper bay, where most of the river input to the bay enters, is dominated by that signal. Both the Lagrangian and Eulerian spatial distributions show marked increase in this region when the river flow was decreased. The western lobe of the upper bay is shallow without much river input and is dominated by the barotropic gyre structure seen in previous studies. It is modulated by the riverine input and by the winds over the bay, but its signature pattern remains even in the harmonics only case.

The best estimate of cell-by-cell residence time from the two methods, is the Lagrangian method. The Eulerian method suffers from an over-smoothing related to the inherent finite size of the grid cells. In contrast, the Lagrangian method tends to concentrate large numbers of particles in regions of low flow, thereby leaving portions of the domain under represented. The Lagrangian method does not suffer however, from numerical diffusion and allows for sub-grid motion that the Eulerian method can only parameterize. The two estimates together though show a strong correlation: the Eulerian concentration-based spatial distribution partitions the bay

into broad regions based on residence time, and the Lagrangian particle accumulation distribution points to sub-regions within the broad Eulerian partition in which to expect shorter or longer residence time.

The forcing parameters varied in the TMDS (i.e., tidal, wind stress, fresh water inflow, and combinations of these) show that the zero sub-tidal change had the smallest effect on the residence time for the bay as well as the smallest effect on the cell-by-cell distributions of residence time compared with the baseline. The zero river run was next in magnitude of effect on bay-wide residence time, but still had a modest effect probably due to the dry winter and spring of 1990-1991. The most profound effect of the more realistic scenarios, was the zero wind run, with a large increase in both the Lagrangian and Eulerian bay-wide residence time, as well as the largest change in the structure of the cell-by-cell residence time spatial distributions of the bay. The harmonics only run and the double mean river input run were both informative as they served as worse case scenarios to bound the bay-wide residence time.

The time series plot (Figure 21) that shows the bay-wide decay to e-folding trend from an exponential decay to an almost linear decrease in normalized concentration or particle accumulation, as the residence time varies from shortest to the longest. This is analogous to the classic drain and fill problem, if a container, full of a marked fluid, is drained constantly at the same rate as it is filled with an unmarked fluid, two extreme situations can occur. The first extreme occurs when perfect instantaneous mixing takes place. The function that describes the amount of

marked fluid at any time t for this situation is $F(t) = Ke^{(bt)}$, where K determines the magnitude at $t = 0$ which is 1 for the normalized concentration here, and b is the ratio of output rate to the volume of the container. The other extreme occurs when the marked and un-marked fluids do not mix at all. The function for this case exhibits a linear trend: $G(t) = K - dt$, where K is the original concentration (again 1 in this case) and d is the ratio of output rate to volume. The long-term mean circulation in the bay can be represented by combining the end members:

$H(t) = Ae^{(bt)} + C(1 - dt)$, with weights A and C , where A determines the magnitude of the exponential contribution; C , the magnitude of the linear contribution. Taking the analogy one step further b and d can be considered to be the ratio of the flow rate out of the bay to bay volume for each weighted component. Using this analogy, the time series in Figure 21 were fit to $H(t)$. The results are shown in Table 8 and Figures 34 - 35.

A gradient-expansion algorithm was used to compute the non-linear least squares fit, until the relative decrease of chi-squared values was less than 0.00001 in one iteration. No exponential function, like $F(t)$, nor any linear function, like $G(t)$, could be fit to every plot at this confidence level. $H(t)$, however, fit all the time series at this level. This does not imply that there is no exponential function fit, only that $H(t)$ provided a better fit.

This expansion into a superposition of functions allows for ranking of all scenarios, with the end members being the almost pure exponential function of the double mean river input case and the nearly linear case of the harmonics only.

Considering only the magnitude coefficients, that is A and C , then the ratio of C to A should indicate which end member is contributing most to the given scenario.

From the analogy, this ratio is in essence a measure of the mixing, or

homogenization over the bay, with high C/A indicating low energy

non-homogenized system and low C/A indicating a high energy well mixed system.

Figure 36 illustrates the variation of residence time with C/A , in particular that it

is a non-linear relationship. The functional relation between residence time and

C/A is given in Figure 37 where a best fit function is plotted over the residence time

verses C/A plot. The nonlinear nature of this function in the region between 2 and

8 on C/A makes comparisons more difficult between widely varying residence times.

Small changes in low values of C/A (less than 2) have large but near-linear effects on residence time, while large changes in high values of C/A are needed to similarly effect the residence time. The change in residence time (RT) with C/A is nearly linear in the range of C/A less than 2 described approximately by

$RT = 155x C/A + 10$ and in the range of C/A greater than 8 described by

$RT = 1.3x C/A + 365$. In these regions, comparisons between scenarios are

simplified by the linear approximation. For example, the C/A value for the double

river input case of the Eulerian method is about 0.16, but for the zero river case it is

1.37. Because the rate of change of RT with C/A in this region is constant (i.e.,

155), the expected increase in residence time from the zero-wind case to the

harmonics-only case from the linear approximation is 188 days (Figure 21). In

comparison, it is calculated to be 183 days from direct integration. Similarly for the

Lagrangian method and the same scenarios, C/A is 0.35 and 1.04, or 106 days (the actual value was 113 days).

The implication here is that anthropogenic impacts to the forces effecting residence time have more influence at lower residence times. Fresh water withdraw from the river sources to the bay, for example, are generally largest during the times of highest flow, which are the periods when the bay has short residence time. These “flushing” periods will be artificially lengthened by the reduction of fresh water input so that wet season values will approach dry season values with a potential for a positive feedback and a cumulative significant lengthening of bay-wide residence time.

Coefficient	A	b	C	d	C/A
Scenario —					
dmr E	0.8875	-0.0175	0.1378	-0.0031	0.155353
bl E	0.4136	-0.0261	0.6175	-0.0022	1.49308
zst E	0.3769	-0.0261	0.6465	-0.0022	1.71522
zr E	0.4343	-0.0208	0.5951	-0.0016	1.37028
zw E	0.0754	-0.0315	0.9163	-0.0024	12.1381
ho E	0.0391	-0.0252	0.9565	-0.0010	24.4512
dmr L	0.7247	-0.0254	0.2569	-0.0022	0.354517
bl L	0.4915	-0.0328	0.4912	-0.0018	0.999406
zst L	0.4616	-0.0341	0.5210	-0.0017	1.12866
zr L	0.4808	-0.0301	0.4986	-0.0014	1.03691
zw L	0.2317	-0.0228	0.7376	-0.0021	3.18366
ho L	0.0543	-0.0571	0.9308	-0.0010	17.1299

TABLE 8. Results of the best fit to $H(t) = Ae^{(bt)} + C(1 - dt)$.

Coefficients for $H(t)$ are given for each scenario and each method, as well as the ratio C/A . The abbreviations denote the scenario, dmr for double mean river input, bl for baseline, zst for zero sub-tidal, zr for zero river input, zw for zero wind, and ho for harmonics only. The E or L denotes whether Eulerian or Lagrangian method.

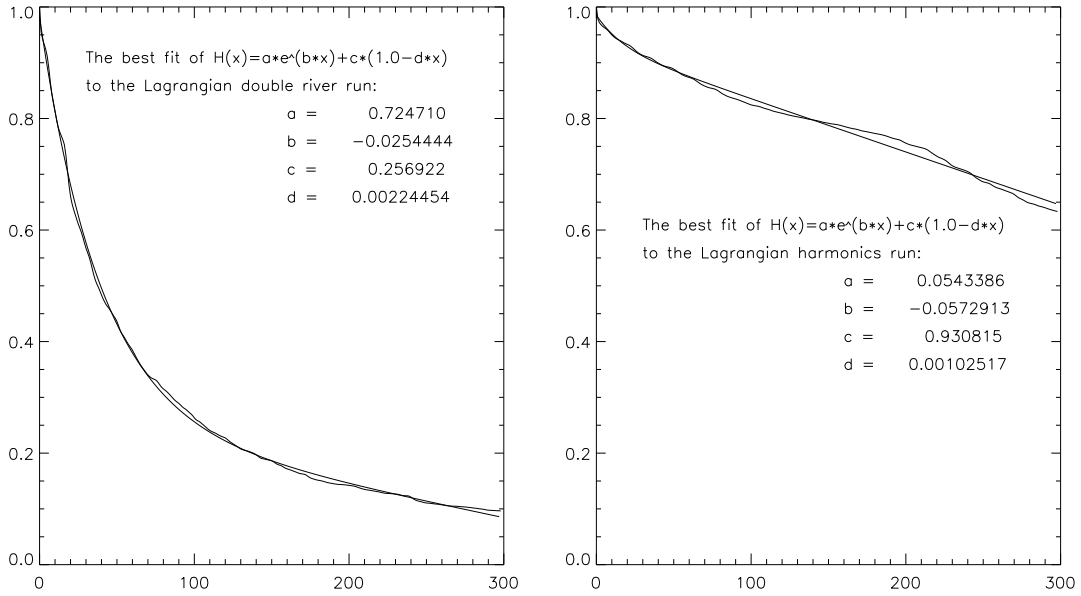


FIG. 34. Lagrangian best fit function for both extremes.

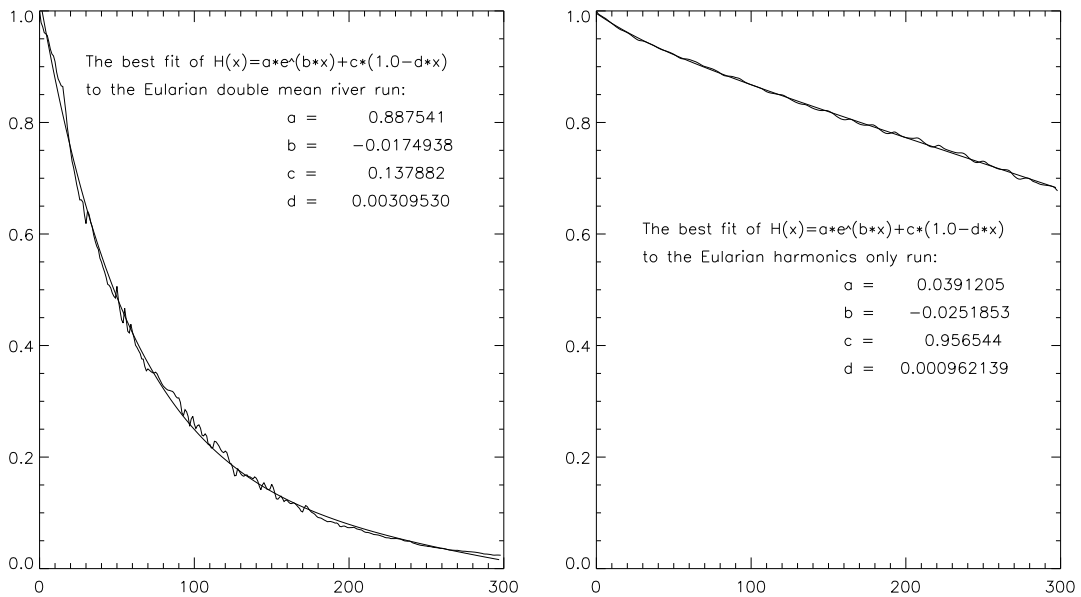


FIG. 35. Eulerian best fit function for both extremes.

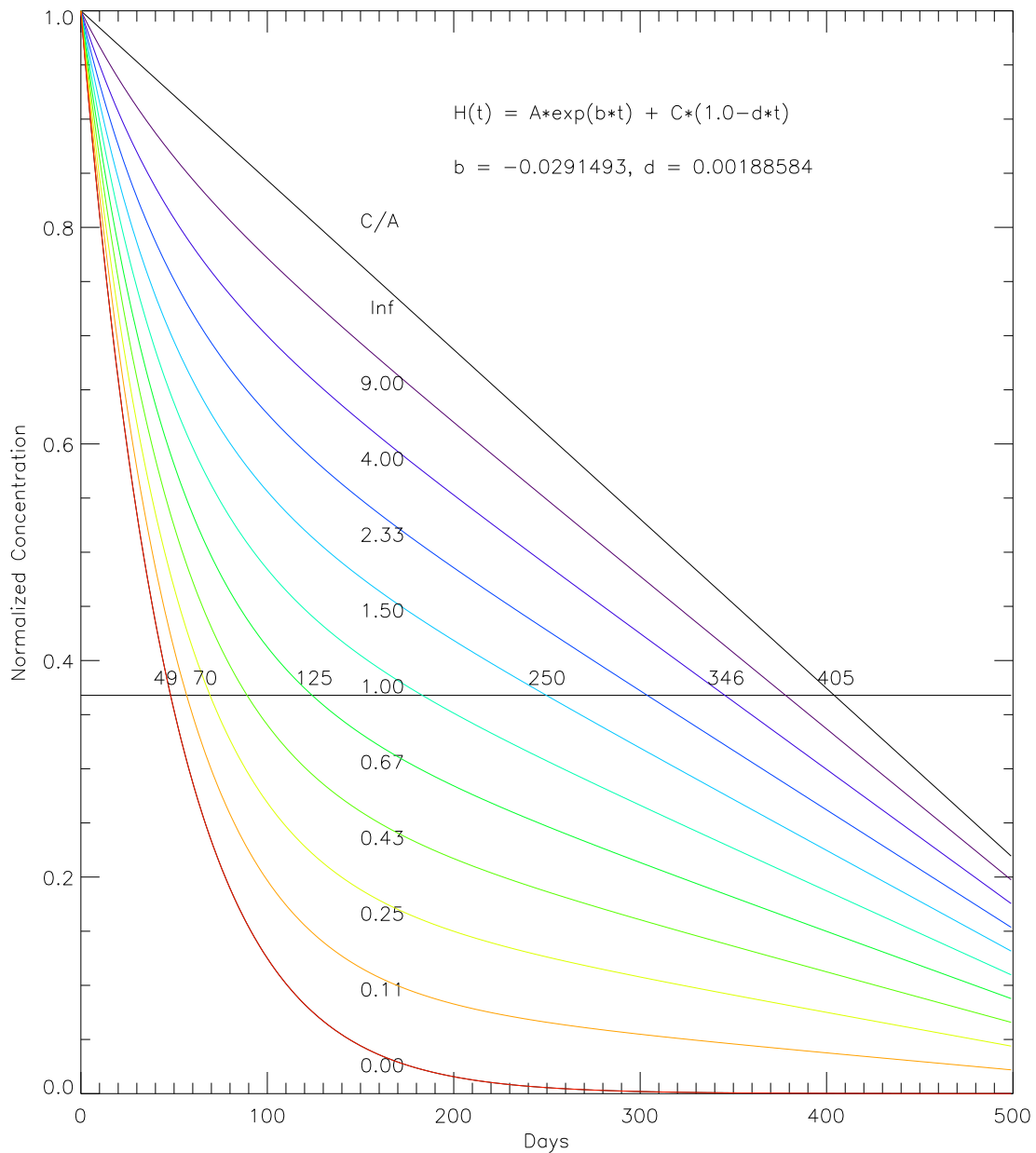


FIG. 36. Time series for theoretical superposition of functions.

The time series of $H(t)$ for various values of C/A , with corresponding residence times. A representative value for b and d was chosen from the best fit $H(t)$ for each case.

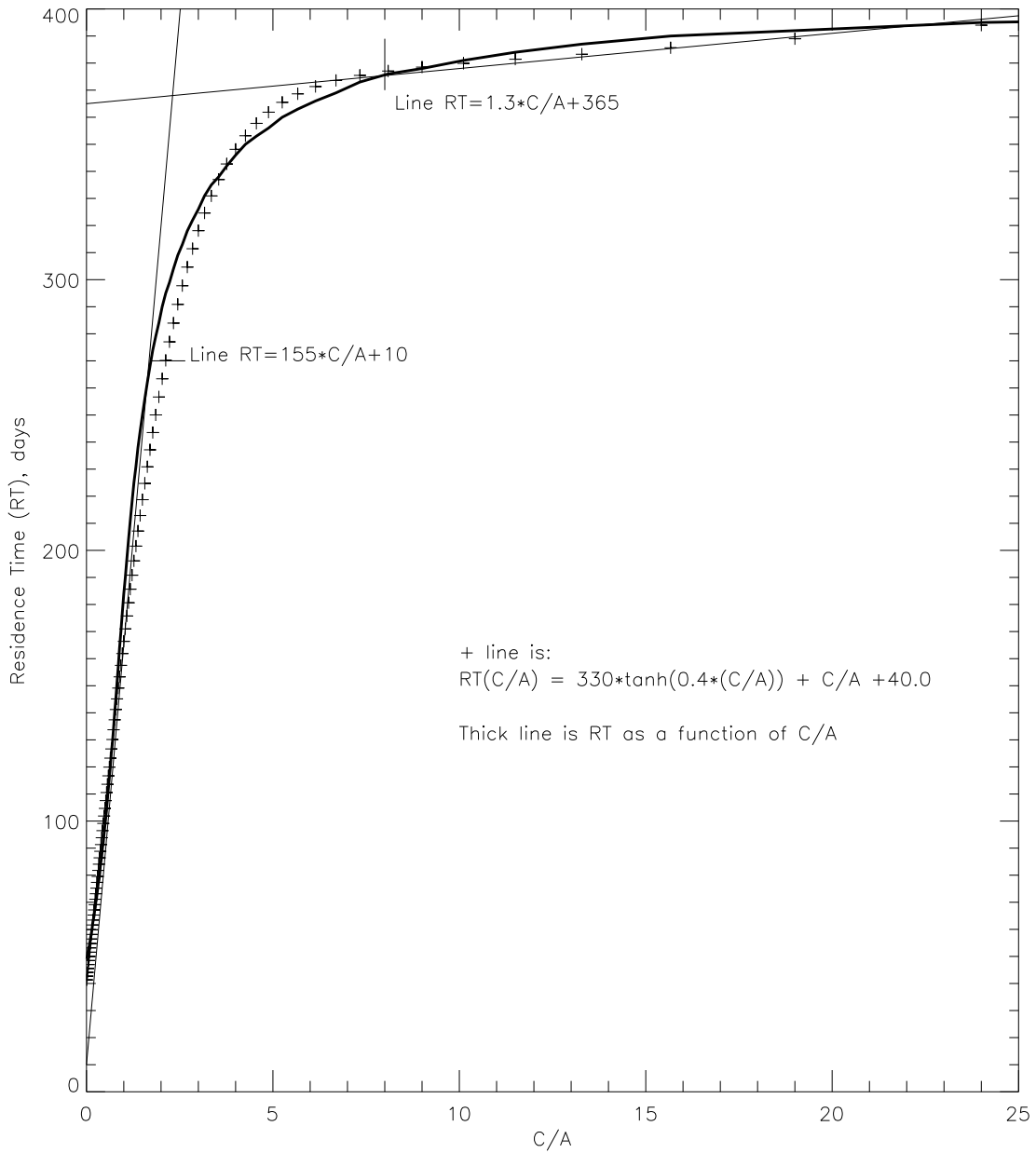


FIG. 37. The functional relation between RT and C/A.

The best fit function $RT(C/A)$ is plotted over the relation between residence time (RT) and the ratio of the coefficients of the liner term and the exponential term (C/A) of $H(t) = Ae^{(bt)} + C(1 - dt)$.

Caveats

There are caveats to the results shown here.

1. The model output is not data and even though great care was taken in validation, the results are a numerical approximation to reality.

2. The particle accumulation is a noisy time series due to the tidal slosh (excursion) that varies from about 10 km near the mouth of the bay at spring tide to almost nill at the edges and in the western lobe of the head of the bay. This was circumvented, in part, by a 7 day running average of the particle accumulation in each grid cell. This smoothing implies the Lagrangian method has an accuracy of +/- 7 days.

3. The Eulerian method is sensitive to the magnitude of the horizontal diffusion coefficient. Changes in this parameter from the SMDS to the TMDS had as big an impact on the bay-wide residence time as did increasing the river input to twice the wet season average, as can be seen by comparison of the cell-by-cell Eulerian plot from the SMDS to the TMDS plot of the double mean river input case.

4. The open boundary looks like an infinite sink of particles or concentration, as it does not allow for particle re-entry or for non-zero concentration input to the domain. This could partially explain the persistent low residence time near the open boundary, and is an unknown at this time.

5. The forcing scenarios do not accurately represent real world conditions. For example, when the river input is set to zero, the open boundary salinities are not varied from the baseline case. In reality, if there were a time with no fresh water

input, the open boundary salinities would most likely rise. The salinities would definitely fall during the double mean river run scenario, but they were fixed to baseline values for that run.

6. The precipitation and evaporation contribute to the overall residual circulation by inputting and extracting fresh water, but were not varied to try to quantify their contribution. They remained at baseline levels for all runs except the harmonics only run where they were set to zero.

7. The vertical mixing of particles was ignored at the sub-grid scale level, under the assumption that isotropic turbulence in the vertical would homogenize the particles in the vertical during high flow periods, and since vertically integrated quantities were all that were considered, the net effect of introducing vertical dispersion would be small. This assumption was not addressed here.

With these caveats in mind, the model is capturing the physics of the flow in the bay as shown in the generally good validation for water levels, velocities, and salinity. The close agreement between the two methods in both bay-wide residence time and general spatial structure, from scenario to scenario, in the cell-by-cell spatial distributions can not be ignored. The differences between the two methods point out that they are both numerical approximations to the true residence time and while each method has merit, together they provide a realistic interpretation of the spatiotemporal structure of the residence time.